Dopamine D2 receptors gate generalization of conditioned threat responses through mTORC1 signaling in the extended amygdala

Dimitri de Bundel, Charleine Zussy, Julie Espallergues, Charles R. Gerfen, Jean-antoine Girault, Emmanuel Valjent

HHS Public Access

Author manuscript

Mol Psychiatry. Author manuscript; available in PMC 2017 January 01.

Published in final edited form as:

Mol Psychiatry. 2016 November ; 21(11): 1545–1553. doi:10.1038/mp.2015.210.

Dopamine D2 receptors gate generalization of conditioned threat responses through mTORC1 signaling in the extended amygdala

Dimitri De Bundel[1,2,3,*], **Charleine Zussy**[1,2,3], **Julie Espallergues**[1,2,3], **Charles R Gerfen**[4], **Jean-Antoine Girault**[5,6,7], and **Emmanuel Valjent**[1,2,3]

[1]CNRS, UMR5203, Institut de Génomique Fonctionnelle, Montpellier, F-34094, France

[2]Inserm, U1191, Montpellier, F-34094, France

[3]Universités de Montpellier, UMR-5203, Montpellier, F-34094, France

[4]Laboratory of Systems Neuroscience, National Institute of Mental Health, Bethesda, Maryland 20892, USA

[5]Inserm, UMR-S 839, F-75005, Paris, France

[6]Institut du Fer à Moulin, F-75005, Paris, France

[7]Sorbonne Universités, UPMC, Université Paris 06 F-75005, Paris, France

Abstract

Overgeneralization of conditioned threat responses is a robust clinical marker of anxiety disorders. In overgeneralization, responses that are appropriate to threat-predicting cues are evoked by perceptually similar safety-predicting cues. Inappropriate learning of conditioned threat responses may thus form an etiological basis for anxiety disorders. The role of dopamine (DA) in memory encoding is well established. Indeed by signaling salience and valence, DA is thought to facilitate discriminative learning between stimuli representing safety or threat. However, the neuroanatomical and biochemical substrates through which DA modulates overgeneralization of threat responses remain poorly understood. Here we report that the modulation of DA D2 receptor (D2R) signaling bidirectionally regulates the consolidation of fear responses. While the blockade of D2R induces generalized fear responses, its stimulation facilitates discriminative learning between stimuli representing safety or threat. Moreover, we show that controlled fear generalization requires the coordinated activation of D2R in the bed nucleus of the stria terminalis (BNST) and the central amygdala (CEA). Finally, we identify the mTORC1 cascade activation as an important molecular event by which D2R mediates its effects. These data reveal that D2R

Correspondence should be addressed to: Emmanuel Valjent, Inserm U1191, CNRS UMR 5203, Institut de Génomique Fonctionnelle, 141 rue de la Cardonille, 34094 Montpellier Cedex 05, France. emmanuel.valjent@igf.cnrs.fr; emmanuel.valjent@gmail.com or Dimitri De Bundel, Dept of Pharmaceutical Chemistry & Drug Analysis, Center for Neurosciences, Vrije Universiteit Brussel, 103 Laarbeeklaan, 1090 Brussels, Belgium. ddebunde@vub.ac.be.

*present address: Department of Pharmaceutical Chemistry and Drug Analysis, Center for Neurosciences, Vrije Universiteit Brussel, 103 Laarbeeklaan, 1090 Brussels, Belgium.

Author contributions

DDB and EV designed the study. DDB conducted experiments and analyzed data. CZ and JE assisted with behavioral experiments. CRG and JAG provided critical reagents and suggestions. DDB and EV wrote the manuscript.

Conflict of interest

The authors declare no competing financial interests.

signaling in the extended amygdala constitutes an important checkpoint through which DA participates in the control of threat processing and the emergence of overgeneralized fear responses.

Introduction

The central extended amygdala is a network of highly interconnected and evolutionary conserved basal forebrain regions controlling behavioral responses towards threatening stimuli (1). Its core components, the central nucleus of the amygdala (CEA) and the bed nucleus of the stria terminalis (BNST), are highly similar in terms of inputs and outputs, and serve complementary roles in the integration of threat-relevant information and the orchestration of fear- and anxiety-related behaviors (1). Whereas the CEA is typically regarded to control phasic fear responses towards specific and imminent threats, the BNST is believed to play a prominent role in anxiety and sustained fear responses towards less specific and less predictable threats (2). However, a more integrated role is likely given that both structures receive monosynaptic inputs from the basolateral amygdala (BLA) and have been implicated in generalization of conditioned threat responses (3–5).

Generalization of threat response is a fundamental behavioral phenomenon described across species and sensory modalities and is proposed to enable the rapid deployment of appropriate defensive strategies during novel encounters of cues resembling those predicting threat (6). However, generalization of threat responses can become excessive, resulting in strong defensive reactions towards cues that do not predict threatening outcomes. Overgeneralization of threat responses is a core feature of anxiety disorders (7) and is believed to result from disrupted memory encoding for threat-predicting stimuli (8). Nevertheless, the neuronal mechanisms governing generalization remain poorly understood, and the molecular substrates through which extended amygdala neurons consolidate adapted behavioral reactions towards potential threats are elusive.

The central extended amygdala receives dense dopamine (DA) inputs originating from the ventral tegmental area (VTA) and the dorsal raphe/periaqueductal grey (DR/PAG) (9). By signaling salience and valence, DA is thought to facilitate discriminative learning of stimuli representing safety and threat (10). Indeed, some DA neurons increase their firing rate in response to aversive stimuli and their predictive cues (11, 12). Moreover, genetic depletion of DA or pharmacological DA receptor blockade prior to conditioning fully disrupts the acquisition of conditioned threat responses (13–16). In contrast, conditional inactivation of N-methyl-D-aspartate (NMDA) receptors in DA neurons and the resulting suppression of DA burst firing following exposure to aversive stimuli yields more subtle effects and was shown to result in generalization of conditioned threat responses (12).

Because of the well-established role of DA in memory consolidation (17–21) we hypothesized that DA may control generalization by ensuring the precise consolidation of conditioned threat responses. Using a mouse behavioral paradigm for auditory threat response generalization, we observed that DA controls generalization through concomitant activation of D2 type receptors (D2R) in both the CEA and BNST. Using the phosphorylation state of the neuronal activation marker ribosomal protein S6 (P-rpS6) (22),

the canonical downstream target of the mTORC1 pathway (23), we found that these effects on consolidation of conditioned aversive behavior were mediated though mTORC1 signaling in the CEA and BNST.

Materials and Methods

Animals and housing

Male 8–12 weeks old C57BL6/J (Charles River Laboratories) and heterozygous BAC-transgenic *Drd2::EGFP* reporter mice (C57BL6/N background, founder S188, GENSAT, Rockefeller University, New York, NY) reporter mice were used in this study (24, 25). Mice were housed in groups of 3–5 to avoid social isolation-induced anxiety and were maintained in a 12 h light/dark cycle under stable laboratory conditions of temperature (22°C) and humidity (60%). Mice were habituated to handling and injection procedures during five consecutive days before experiments. All experiments were in accordance with the guidelines of the French Agriculture and Forestry Ministry for handling animals (C34-172-13).

Intracerebral cannula implantation

Mice were anesthetized with a mixture of ketamine (Imalgene 500, 50 mg/ml, Merial), 0.9% (w/v) NaCl solution (saline) and xylazine (Rompun 2%, 20 mg/ml, Bayer) (2:2:1, i.p., 0.1 ml/30 g) and mounted on a stereotaxic apparatus using flat skull coordinates (26). Stainles steel guide cannulae (26 gauge, 5.00 mm, Plastics One) were implanted 0.5 mm above the CEl (A/P = −1.34 mm; M/L = 2.90 mm; D/V = −4.25 mm) or BNSTov (A/P = +0.2 mm; M/L = 2.0 mm; D/V = −3.50 mm). CEl cannulae were implanted vertically whereas BNSTv cannulae were implanted under a 15° angle towards midline in the coronal plane to avoid damage to the wall of the lateral ventricle. The guide cannulae were fixed to the skull with anchor screws and dental acrylic (AgnTho's). Following surgery, mice were placed on a heating pad and a dummy cannula was screwed in the guide cannula to seal off the opening. Mice were allowed to recover for a minimum of 7 days prior to behavioral testing.

Systemic drug administration

In the experiments with systemic drug administration, SKF81297 (5.0 mg/kg, i.p.), SCH23390 (0.1 mg/kg), quinpirole (1.0 mg/kg, i.p.) and raclopride (0.3 mg/kg, i.p.) were dissolved in 0.9% (w/v) NaCl (saline) and injected immediately following conditioning. The used doses of DA receptor ligands were chosen based on previous studies showing *in vivo* regulation of DA signaling responses (27–29). Rapamycin (5.0 mg/kg) was solubilized in a mixture of 5% (v/v) DMSO, 5% (v/v) Tween 80 and 15% (v/v) PEG-400 in water and was injected once daily starting three days before the final injection immediately following fear conditioning. This protocol was previously shown to selectively block mTORC1 signaling (30, 31). Control mice were injected with the appropriate vehicle at the corresponding time point. The injected volume was 0.1 ml per 10 g bodyweight for all drugs except for rapamycin, for which the injected volume was 0.05 ml per 10 g bodyweight. All drugs were purchased from Tocris.

Intracranial drug infusion

In the experiments with intracerebral drug administration, raclopride (1 mg/ml, 0.5 μg per hemisphere) was dissolved in 0.9% (w/v) NaCl solution and infused immediately following conditioning and rapamycin (2 mg/ml, 1 μg per hemisphere) was dissolved in DMSO. The used dose of raclopride was chosen based on a previous study demonstrating regulation of anxiety-related behavior upon infusion in the amygdala (32). Similarly, the used dose of rapamycin was previously shown to modulate fear memory consolidation upon infusion in the amygdala (33). Control mice were infused with the appropriate vehicle at the same time point. Mice were gently hold by the scruff and the infusion cannula was inserted into the guide cannula. The tip of the infusion cannula protrudes 0.5 mm from the tip of the guide cannula, thus penetrating the brain site of interest. Infusions were made at a flow rate of 0.5 μl/min. A total volume of 0.5 μl was infused in each site. Following infusion, the infusion cannula was left in place for 1 min to enable diffusion of drugs and to avoid liquid reflux through the guide cannula.

Fear conditioning

The experiments were carried out in a fear conditioning apparatus comprising a test box (20 cm width × 20 cm length × 20 cm height) placed within a sound proof chamber (Panlab, Harvard Apparatus). Two different contextual configurations were used (A: square configuration, white walls, white rubber floor, washed with 70% ethanol; B: circular insert, black walls, metal grid on black floor, washed with 1% acetic acid). On day 1, mice are subjected to a habituation session in context A. After 2 min of habituation to the box, they were exposed to 5 alternating presentations of two different tones (2.5 or 7.5 kHz, 85 dB, 30 s). The interval between tone presentations during the habituation session was randomized between 20–120 s. On day 2, discriminative fear conditioning was performed in context B. After 2 min habituation to the box, animals received 5 pairings of one tone (CS+, semi-randomly assigned as 2.5 or 7.5 kHz, counterbalanced between mice across experimental groups) with an unconditioned stimulus (US: 0.6 mA scrambled footshock, 2 s, coinciding with the last 2 s of CS+ presentation). The other tone (CS−) was presented intermittently, following each pairing of the CS+ with the US, but never coinciding with the US. The interval between CS+ and CS− presentations during the conditioning session was randomized between 20–120 s. On day 3, conditioned mice are submitted to fear retrieval in context A. After 1 min habituation to the box, mice received presentations of the CS− or CS + in a block of 4 with 20–120 s interval followed 4 h later by 1 min habituation to the box and 4 presentations of the CS+ or CS− in a block of 4 with 20–120 s interval. The order in which the CS+ and the CS− were presented was counterbalanced across animals. Freezing behavior during CS+ and CS− presentations was analyzed using a load cell coupler (Panlab, Barcelona, Spain) and was defined as the lack of activity above a calibrated threshold for a duration of 2 s or more as determined with the Freezing software (Panlab, Barcelona, Spain). The average time spent freezing prior to presentation of the sounds during both test sessions (Pre) was used as a measure for contextual fear generalization. Mice were randomly assigned to experimental groups.

Tissue preparation and immunofluorescence

Mice were rapidly anaesthetized with pentobarbital (500 mg/kg, i.p., Sanofi-Aventis, France) and transcardially perfused with 4% (w/v) paraformaldehyde in 0.1 M sodium phosphate buffer (pH 7.5) (34). Brains were post-fixed overnight in the same solution and stored at 4°C. Fourty μm-thick sections were cut with a vibratome (Leica, France) and stored at −20°C in a solution containing 30% (v/v) ethylene glycol, 30% (v/v) glycerol, and 0.1 M sodium phosphate buffer, until they were processed for immunofluorescence (35). Sections were processed as follows: free-floating sections were rinsed three times 10 min in Tris-buffered saline (50 mM Tris-HCL, 150 mM NaCl, pH 7.5). For PKCδ immunofluorescence staining an antigen-retrieval protocol was applied. Following the initial TBS rinse, sections were incubated for 15 min at 75°C in a buffer containing 10 mM Citrate and 0.05% Tween20 at Ph 6.5. Next sections were rinsed three times in TBS. Sections were then permeabilized and blocked in a solution containing 3% BSA (w/v) and 0.3% (v/v) Triton X-100 in TBS and incubated for 72 hrs at 4°C in 1% BSA (w/v), 0.1% (v/v) Triton X-100 with the primary antibodies. The following primary antibodies were used: chicken anti-GFP (1:500, Life Technologies, A10262), rabbit anti-pS235/236-rpS6 (1:500, Cell Signaling Technologies, 2211), and mouse anti-PKCδ (1:500, BD Transduction Laboratories, 610398). Following primary antibody incubation, sections were rinsed three times for 10 min in TBS and incubated for 45 min at room temperature with goat Cy2-, Cy3- or Cy5-coupled secondary antibodies (1:500, Jackson Immunoresearch). Sections were rinsed for 10 min twice in TBS and twice in Tris-buffer (1 M, pH 7.5) before mounting in 1,4-diazabicyclo-[2. 2. 2]-octane (DABCO, Sigma-Aldrich).

Confocal microscopy and image analysis were carried out at the Montpellier RIO Imaging Facility. Images from each region of interest were single confocal sections obtained using sequential laser scanning confocal microscopy (Zeiss LSM780). Photomicrographs were obtained with the following band-pass and long-pass filter setting: Cy2 (band pass filter: 505–530), Cy3 (band pass filter: 560–615), and Cy5 (long-pass filter 650). Images used for quantification were all single confocal sections. The objectives and the pinhole setting (1 airy unit) remain unchanged during the acquisition of a series for all images within an experiment. The thickness of the optical section is ~1.6 μm with a 20× objective and ~6 μm with a 10× objective. P-rpS6-positive cells were quantified in zones or regions of the same area corresponding to the CEl or BNSTov. Quantification of immunoreactive cells was performed blinded to experimental conditions using the cell counter plugin of the ImageJ software taking as standard reference a fixed threshold of fluorescence.

Statistical analysis

Values are expressed as means ± s.e.m. Statistical analysis was performed by one-way or two-way ANOVA (with matching for repeated measures (RM) as indicated) followed by Tukey post-hoc comparisons.

Results

Bidirectional modulation of conditioned threat response generalization by D2R

We studied the molecular mechanisms controlling threat memory generalization, using a protocol in which mice learn to distinguish between two auditory cues (conditioned stimulus, CS) associated (CS+) or not (CS−) with a threat. After habituation (without shock) to the CS+ and CS− in context A (day 1), mice were conditioned in context B (day 2). During the conditioning, CS+ was specifically associated with an unconditioned stimulus (US), a footshock. The CS− was presented during the same training session but never associated with a footshock (Figure 1a). CS+ and CS− were presented 5 times during a 15-min session (Figure 1a and Supplemental Figure 1). On day 3 (context A), mice were re-exposed to one type of cue followed, 4 h later, by re-exposure to the other type of cue. Freezing was measured as the typical threat response (Figure 1a, b). Following conditioning, mice displayed high freezing levels after CS+ presentation (Figure 1b). Although less pronounced, a significant freezing response was also observed following CS− presentation suggesting a certain degree of fear generalization (Figure 1b). To determine whether DA participates in the consolidation of this form of discriminative learning, dopamine D1R and D2R agonists and antagonists were injected immediately after conditioning and mice were tested the following day in a drug-free state (Figure 1a). Neither blockade (SCH23390, 0.1 mg/kg, i.p.) nor stimulation (SKF81297, 5 mg/kg, i.p.) of D1R altered the learned fear responses (Figure 1b). In contrast, modulation of D2R bidirectionally regulated the consolidation of fear responses: mice treated with a D2R antagonist, raclopride (0.3 mg/kg, i.p.), displayed equivalent freezing response to both CS+ and CS− (Figure 1b). Conversely, stimulation of D2R by quinpirole (1 mg/kg, i.p.) tended to enhance discrimination between CS+ and CS− (Figure 1b). This was confirmed when mice were conditioned at a high footshock intensity of 1 mA, after which saline-treated mice showed generalization, whereas quinpirole-treated mice showed clearly different behavioral responses towards CS+ and CS− (Figure 1c). Together these results suggested that DA gates the discrimination of cues previously associated with different value through D2R.

CEA D2R control fear generalization

Although D2R binding sites have been detected in the CEA (32), the identity of D2R-containing neurons in this brain area remains elusive. We therefore analyzed the anatomical distribution of D2R-expressing cells in the CEA by using *Drd2::EGFP* mice. The analysis of GFP expression revealed that D2R-expressing neurons were predominantly found in the lateral part of the CEA (CEl) and to a lesser extent in the medial part of the CEA (CEm) (Figure 2a, b). Double immunofluorescence analysis revealed that most CEl D2R-expressing cells were PKCδ-immunoreactive, a marker previously shown to identify GABAergic neurons in this brain region (5) (Figure 2c, d).

To investigate whether CEA could be a target of DA activated by aversive stimuli, we monitored P-rpS6 1 and 2 h after the end of the conditioning session. At 1 h we found an increase in P-rpS6 in the CEl of mice subjected to five CS+US pairings compared to control mice only exposed to the CS (Supplemental Figure 2a, b). In the CEl, increased P-rpS6 was specific towards $PKC\delta^{+}$ cells and was prevented when raclopride was injected after

conditioning (Figure 2e, f). Moreover, the administration of quinpirole increased P-rpS6 in CEl PKCδ$^+$ cells (Figure 2g and Supplemental Figure 3a, b). Together these results indicated that both aversive conditioning and pharmacological stimulation of D2R activated CEl PKCδ$^+$ neurons.

To determine whether D2R located in the CEA participate in the control of fear generalization, mice were implanted bilaterally with cannulas in the CEA (Figure 2h and Supplemental Figure 4). Mice infused bilaterally with raclopride into the CEA immediately following conditioning showed generalized freezing responses when re-exposed to CS+ and CS− 24 h later (Figure 2i). Taken together, these data suggest that the stimulation of D2R in the CEA is required to prevent generalization of threat responses.

Blockade of BNST D2R induces fear generalization

The BNST was previously shown to have a high density of D2R (36), but as for the CEA, the identity of D2R-containing cells in this brain area is not known. We therefore used *Drd2::EGFP* mice to characterize the distribution of D2R-expressing cells in the BNST (Figure 3a). We found that GFP-containing cells were distributed throughout the BNST, with the highest density in the oval nucleus of the BNST (BNSTov) (Figure 3b). Reminiscent of our observations in the CEl, a high proportion of D2R-expressing BNSTov neurons co-expressed PKCδ (~84%) (Figure 3c, d). As observed in the CEA, aversive conditioning increased the phosphorylation of rpS6 in the BNST (Supplemental Figure 5a, b), mainly in BNSTov PKCδ$^+$ cells and required D2R stimulation (Figure 3e, f). In addition, the administration of quinpirole also increased P-rpS6 in the BNSTov PKCδ$^+$ cells (Figure 3g and Supplemental Figure 6a, b) indicating that similarly to CEl PKCδ$^+$ neurons BNSTov PKCδ$^+$ cells are also highly responsive to aversive conditioning and pharmacological stimulation of D2R.

We therefore tested whether the modulation of D2R located in the BNST affected fear generalization. Mice bilaterally infused with raclopride into the BNST immediately following conditioning displayed equivalent freezing responses during CS+ and CS− presentation the following day (Figure 3h, i and Supplemental Figure 7), demonstrating their inability to discriminate between cues predicting relative safety and threat. Together these observations suggested that D2R in the BNST exerts a role highly similar to that of D2R in the CEA in controlling generalization of threat responses.

Coordinated activation of D2R in the CEA and BNST prevents fear generalization

The concomitant activation of CEl and BNSTov PKCδ$^+$ neurons following aversive conditioning led us to investigate whether the coordinated stimulation of D2R in the CEA and the BNST is required to prevent generalization of freezing responses. To test this hypothesis, we performed a pharmacological disconnection of these structures by injecting raclopride into the CEA in one hemisphere and into BNST in the other hemisphere (Figure 4). While the blockade of D2R in CEA on one side of the brain and in BNST on the other side (i.e. disconnection) induced generalized freezing responses (Figure 4a and Supplemental Figure 8a), the ipsilateral blockade of D2R in the two regions did not impact on the discrimination between CS+ and CS− (Figure 4b and Supplemental Figure 8b). This

result indicated that the concomitant recruitment of both structures is required to control threat response generalization.

mTORC1 inhibition prevents rpS6 phosphorylation and induces overgeneralization

Among the various protein kinases involved in rpS6 phosphorylation, the canonical pathway mammalian target of rapamycin complex 1 (mTORC1)/p70 ribosomal protein S6 kinases 1 and 2 (p70S6K1/2) plays a prominent role (37). We therefore tested whether the mTORC1 pathway was involved in the regulation of P-rpS6 in PKCδ^{+} BNSTov and CEl neurons following aversive Pavlovian conditioning. While vehicle-treated mice showed an increase of P-rpS6 in the CEl (Figure 5a, b) and BNSTov (Figure 5c, d), the state of phosphorylation of rpS6 was unchanged in both structures in mice pretreated with a low dose of the mTORC1 inhibitor rapamycin (5 mg/kg, i.p.). Similarly, quinpirole-induced P-rpS6 in PKCδ^{+} BNSTov and CEl cells was strongly decreased in rapamycin-treated mice (Supplemental Figure 9).

To determine whether mTORC1 activation in the extended amygdala participated in the control of fear generalization, two cohorts of mice were implanted bilaterally with cannulas either in the CEA or in the BNST (Figure 5e, f). Bilateral infusion of rapamycin into the CEA immediately after conditioning induced a general impairment of conditioned threat learning since freezing responses evoked by the CS+ were significantly diminished compared to saline (Figure 5e). On the other hand, bilateral infusion of rapamycin into the BNST selectively disrupted discriminative learning as evidenced by the pronounced increase in freezing responses during CS− presentation, which became indistinguishable from CS+ presentation (Figure 5f). Altogether, these results suggest that mTORC1 activation in the extended amygdala controls consolidation of threat memory.

Discussion

Previous pharmacological and genetic studies have suggested a role of DA in the stabilization of aversive memory traces and in the modulation of threat response generalization (12, 38). Generalization is controlled at different anatomical checkpoints throughout the fear circuit including the prefrontal cortex (39, 40), the lateral amygdala (8, 41), and the extended amygdala (3–5). Here we demonstrate that DA facilitates the consolidation of appropriate behavioral threat responses in mice following auditory fear conditioning through concomitant D2R activation in the CEA and BNST. Importantly, our results show that D2R signaling coordinates mTORC1 activation in these two extended amygdala structures that are often considered as largely independent but complementary systems involved in fear and anxiety processing (2).

The CEA has a well-established role in the acquisition, consolidation and expression of fear responses towards auditory threat-predicting cues (CS+) (3, 42, 43) but was also found to be involved in generalization of fear responses towards non-predictive auditory cues (CS−) (3, 5). The BNST, however, does not appear to be critically involved in CS+ fear responses (44), but nevertheless controls generalization towards CS− fear responses (4). Supporting their involvement in generalization, both extended amygdala substructures have been shown to contribute to anxiety-like behaviors (45–47). The CEA and BNST have strong reciprocal

connections (48, 49) and receive direct glutamatergic inputs from the BLA (46, 47). Moreover, their output towards the brainstem displays a surprising level of temporal coordination in response to BLA stimulation (50, 51). Indeed, both the CEA and BNST project towards the ventrolateral PAG (PAGvl), the brainstem region controlling freezing behavior, suggesting that cooperation of extended amygdala outputs maximizes control over conditioned threat responses.

The extended amygdala receives DA inputs from the VTA and the DR/PAG (9). The VTA inputs are spread diffusely over the CEA and BNST, whereas the DR/PAG inputs are highly focalized on the CEl and BNSTov (52). The existence of D2R in the CEA and BNST was previously reported using immunohistochemistry and receptor autoradiography approaches (32, 36, 53). Extending these previous observations, our analysis revealed that D2R-expressing neurons were mainly distributed in the CEl and BNSTov and that a large majority of them also expressed PKCδ (78% for the CEl and 84% for the BNSTov). The presence of D2R was further supported by the ability of quinpirole, a D2R agonist, to enhance rpS6 phosphorylation in CEl and BNST PKCδ$^+$ neurons. However, one cannot exclude that the observed effects on rpS6 phosphorylation in PKCδ$^+$ cells are the integrated result of D2R modulation within neuronal circuits of the CEA and BNST. Indeed, in addition to their expression in CEA and BNST PKCδ-expressing neurons, D2R are also found at presynaptic levels where they could participate to disinhibition in the extended amygdala circuit by decreasing GABA release therefore facilitating the activation of CEl and BNSTov PKCδ$^+$ neurons (36, 54, 55).

We found that aversive conditioning increased the P-rpS6 in CEl and BNSTov PKCδ$^+$ cells through the stimulation of D2R. Interestingly, systemic or local infusion of raclopride immediately following fear conditioning into the CEA or BNST elicited threat response generalization. This suggests that activation of PKCδ$^+$ cells following aversive conditioning prevents threat response generalization whereas interventions that prevent activation of PKCδ$^+$ cells elicit generalization. Interestingly, CEl PKCδ$^+$ cells are inhibited by CEl somatostatin-immunoreactive (SOM$^+$) cells (3, 56) and fear conditioning with a high intensity foot shock (1 mA) was previously shown to cause increased excitatory synaptic transmission onto SOM$^+$ cells and thereby weakening that onto PKCδ$^+$ cells (42). In our experiments, similar training conditions elicited threat response generalization, suggesting that this phenomenon may result from shifts in synaptic strength between SOM$^+$ cells and PKCδ$^+$ cells. Indeed, we found that the stimulation of D2R not only increased phosphorylation of rpS6 specifically in PKCδ$^+$ cells of the extended amygdala and but also prevented fear generalization induced by conditioning with a high-intensity foot shock. In line with our results, pharmacogenetic silencing of CEl PKCδ$^+$ cells during fear conditioning and subsequent testing was previously shown to increase freezing responses both during and after auditory cue presentation, suggesting generalization (5). Moreover, optogenetic activation of CEl PKCδ$^+$ cells was shown to be anxiolytic (57). Interestingly, a recent study demonstrated that optogenetic activation of CEl PKCδ$^+$ cells during retrieval of fear memory was anxiogenic and promoted fear generalization (58). This apparent contradiction may reflect the dual role of CEA in both incentive salience and valence (59). Further investigation will be necessary to determine whether BNSTov and CEl PKCδ$^+$ cells signals salience and/or valence.

Several studies previously demonstrated the role of mTORC1 signaling in fear memory consolidation (33, 60–62). Indeed, the blockade of mTORC1 disrupted consolidation of auditory CS+ fear responses (60, 61). Our present findings demonstrate that the increase in rpS6 phosphorylation in extended amygdala PKCδ$^+$ cells following fear conditioning or D2R activation required mTORC1 activation raising the possible role of mTORC1 in the control of fear generalization. Supporting this hypothesis, the injection of rapamycin into the BNST disrupted the discrimination between CS+ and CS− without affecting the consolidation of CS+ freezing responses. On the other hand, local administration of rapamycin in the CEA impaired the consolidation of conditioned threat responses to both CS + and CS−. The most parsimonious explanation for such results is that infused rapamycin reached the adjacent LA/BlA complex, where inhibition of mTORC1 signaling was previously shown to disrupt the consolidation of CS+ freezing responses (33). Although genetic approaches will be necessary to determine the contribution of CEA mTORC1 signaling in fear generalization, these findings indicate that in the BNST mTORC1 signaling plays a role in the prevention of excessive fear generalization.

In conclusion, we identified D2R as a critical modulator of threat response generalization. We found that D2R activation prevents excessive generalization through mTORC1 signaling in PKCδ$^+$ cells of the extended amygdala. Our data add to the growing body of evidence showing that appropriate behavioral responses to threats require a highly orchestrated cooperation between the CEA and BNST (1). Over time, transitions from phasic fear to sustained fear and anxiety-related behaviors may be reflected by an anatomical shift from the CEA to BNST. However, during the initial consolidation of conditioned threat responses, both extended amygdala substructures are critically involved. These findings provide insights into a potential etiological mechanism and core feature of anxiety disorders.

Supplementary Material

Refer to Web version on PubMed Central for supplementary material.

Acknowledgments

We thank members of the Valjent laboratory for discussions. We also thank Dr Bo Li for insightful and constructive comments. This work was supported by Inserm (ATIP-Avenir), and the *Agence Nationale de la Recherche* (ANR-2010-JCJC-1412) to EV. DDB was a recipient of a postdoctoral fellowship from the *Fondation pour la Recherche Médicale* (FRM). JAG is supported by an ERC Advanced Grant and is affiliated with the Paris School of Neuroscience and the Bio-Psy Laboratory of excellence.

References

1. Fox AS, Oler JA, Tromp do PM, Fudge JL, Kalin NH. Extending the amygdala in theories of threat processing. Trends Neurosci. 2015 May; 38(5):319–29. [PubMed: 25851307]
2. Davis M, Walker DL, Miles L, Grillon C. Phasic vs sustained fear in rats and humans: role of the extended amygdala in fear vs anxiety. Neuropsychopharmacology. 2010 Jan; 35(1):105–35. [PubMed: 19693004]
3. Ciocchi S, Herry C, Grenier F, Wolff SB, Letzkus JJ, Vlachos I, et al. Encoding of conditioned fear in central amygdala inhibitory circuits. Nature. 2010 Nov 11; 468(7321):277–82. [PubMed: 21068837]
4. Duvarci S, Bauer EP, Pare D. The bed nucleus of the stria terminalis mediates interindividual variations in anxiety and fear. J Neurosci. 2009 Aug 19; 29(33):10357–61. [PubMed: 19692610]

5. Haubensak W, Kunwar PS, Cai H, Ciocchi S, Wall NR, Ponnusamy R, et al. Genetic dissection of an amygdala microcircuit that gates conditioned fear. Nature. 2010 Nov 11; 468(7321):270–6. [PubMed: 21068836]
6. Dunsmoor JE, Paz R. Fear Generalization and Anxiety: Behavioral and Neural Mechanisms. Biol Psychiatry. 2015 Sep 1; 78(5):336–43. [PubMed: 25981173]
7. Lissek S, Powers AS, McClure EB, Phelps EA, Woldehawariat G, Grillon C, et al. Classical fear conditioning in the anxiety disorders: a meta-analysis. Behav Res Ther. 2005 Nov; 43(11):1391–424. [PubMed: 15885654]
8. Ghosh S, Chattarji S. Neuronal encoding of the switch from specific to generalized fear. Nat Neurosci. 2015 Jan; 18(1):112–20. [PubMed: 25436666]
9. Hasue RH, Shammah-Lagnado SJ. Origin of the dopaminergic innervation of the central extended amygdala and accumbens shell: a combined retrograde tracing and immunohistochemical study in the rat. J Comp Neurol. 2002 Dec 2; 454(1):15–33. [PubMed: 12410615]
10. Bromberg-Martin ES, Matsumoto M, Hikosaka O. Dopamine in motivational control: rewarding, aversive, and alerting. Neuron. 2010 Dec 9; 68(5):815–34. [PubMed: 21144997]
11. Joshua M, Adler A, Mitelman R, Vaadia E, Bergman H. Midbrain dopaminergic neurons and striatal cholinergic interneurons encode the difference between reward and aversive events at different epochs of probabilistic classical conditioning trials. J Neurosci. 2008 Nov 5; 28(45): 11673–84. [PubMed: 18987203]
12. Zweifel LS, Fadok JP, Argilli E, Garelick MG, Jones GL, Dickerson TM, et al. Activation of dopamine neurons is critical for aversive conditioning and prevention of generalized anxiety. Nat Neurosci. 2011 May; 14(5):620–6. [PubMed: 21499253]
13. Fadok JP, Dickerson TM, Palmiter RD. Dopamine is necessary for cue-dependent fear conditioning. J Neurosci. 2009 Sep 9; 29(36):11089–97. [PubMed: 19741115]
14. Greba Q, Gifkins A, Kokkinidis L. Inhibition of amygdaloid dopamine D2 receptors impairs emotional learning measured with fear-potentiated startle. Brain Res. 2001 Apr 27; 899(1–2):218–26. [PubMed: 11311883]
15. Guarraci FA, Frohardt RJ, Falls WA, Kapp BS. The effects of intra-amygdaloid infusions of a D2 dopamine receptor antagonist on Pavlovian fear conditioning. Behav Neurosci. 2000 Jun; 114(3): 647–51. [PubMed: 10883814]
16. Guarraci FA, Frohardt RJ, Young SL, Kapp BS. A functional role for dopamine transmission in the amygdala during conditioned fear. Ann N Y Acad Sci. 1999 Jun 29.877:732–6. [PubMed: 10415694]
17. Gonzalez MC, Kramar CP, Tomaiuolo M, Katche C, Weisstaub N, Cammarota M, et al. Medial prefrontal cortex dopamine controls the persistent storage of aversive memories. Front Behav Neurosci. 2014; 8:408. [PubMed: 25506318]
18. Gozzani JL, Izquierdo I. Possible peripheral adrenergic and central dopaminergic influences in memory consolidation. Psychopharmacology (Berl). 1976 Aug 26; 49(1):109–11. [PubMed: 822441]
19. Lalumiere RT, Nguyen LT, McGaugh JL. Post-training intrabasolateral amygdala infusions of dopamine modulate consolidation of inhibitory avoidance memory: involvement of noradrenergic and cholinergic systems. Eur J Neurosci. 2004 Nov; 20(10):2804–10. [PubMed: 15548223]
20. Manago F, Castellano C, Oliverio A, Mele A, De Leonibus E. Role of dopamine receptors subtypes, D1-like and D2-like, within the nucleus accumbens subregions, core and shell, on memory consolidation in the one-trial inhibitory avoidance task. Learn Mem. 2009 Jan; 16(1):46–52. [PubMed: 19117916]
21. Maroun M, Akirav I. Differential involvement of dopamine D1 receptor and MEK signaling pathway in the ventromedial prefrontal cortex in consolidation and reconsolidation of recognition memory. Learn Mem. 2009 Apr; 16(4):243–7. [PubMed: 19318466]
22. Knight ZA, Tan K, Birsoy K, Schmidt S, Garrison JL, Wysocki RW, et al. Molecular profiling of activated neurons by phosphorylated ribosome capture. Cell. 2012 Nov 21; 151(5):1126–37. [PubMed: 23178128]
23. Shimobayashi M, Hall MN. Making new contacts: the mTOR network in metabolism and signalling crosstalk. Nat Rev Mol Cell Biol. 2014 Mar; 15(3):155–62. [PubMed: 24556838]

24. Gerfen CR, Paletzki R, Heintz N. GENSAT BAC cre-recombinase driver lines to study the functional organization of cerebral cortical and basal ganglia circuits. Neuron. 2013 Dec 18; 80(6): 1368–83. [PubMed: 24360541]
25. Valjent E, Bertran-Gonzalez J, Herve D, Fisone G, Girault JA. Looking BAC at striatal signaling: cell-specific analysis in new transgenic mice. Trends Neurosci. 2009 Oct; 32(10):538–47. [PubMed: 19765834]
26. Franklin K, Paxinos G. The Mouse Brain in Stereotaxic Coordinates, 3rd ed. Elsevier. 2007
27. Bertran-Gonzalez J, Hakansson K, Borgkvist A, Irinopoulou T, Brami-Cherrier K, Usiello A, et al. Histone H3 phosphorylation is under the opposite tonic control of dopamine D2 and adenosine A2A receptors in striatopallidal neurons. Neuropsychopharmacology. 2009 Jun; 34(7):1710–20. [PubMed: 19158668]
28. Gangarossa G, Perroy J, Valjent E. Combinatorial topography and cell-type specific regulation of the ERK pathway by dopaminergic agonists in the mouse striatum. Brain Struct Funct. 2013 Mar; 218(2):405–19. [PubMed: 22453353]
29. Gangarossa G, Espallergues J, de Kerchove d'Exaerde A, El Mestikawy S, Gerfen CR, Herve D, et al. Distribution and compartmental organization of GABAergic medium-sized spiny neurons in the mouse nucleus accumbens. Front Neural Circuits. 2013; 7:22. [PubMed: 23423476]
30. Huynh TN, Santini E, Klann E. Requirement of Mammalian target of rapamycin complex 1 downstream effectors in cued fear memory reconsolidation and its persistence. J Neurosci. 2014 Jul 2; 34(27):9034–9. [PubMed: 24990923]
31. Santini E, Heiman M, Greengard P, Valjent E, Fisone G. Inhibition of mTOR signaling in Parkinson's disease prevents L-DOPA-induced dyskinesia. Sci Signal. 2009; 2(80):ra36. [PubMed: 19622833]
32. Perez de la Mora M, Gallegos-Cari A, Crespo-Ramirez M, Marcellino D, Hansson AC, Fuxe K. Distribution of dopamine D(2)-like receptors in the rat amygdala and their role in the modulation of unconditioned fear and anxiety. Neuroscience. 2012 Jan 10.201:252–66. [PubMed: 22100273]
33. Parsons RG, Gafford GM, Helmstetter FJ. Translational control via the mammalian target of rapamycin pathway is critical for the formation and stability of long-term fear memory in amygdala neurons. J Neurosci. 2006 Dec 13; 26(50):12977–83. [PubMed: 17167087]
34. Valjent E, Pascoli V, Svenningsson P, Paul S, Enslen H, Corvol JC, et al. Regulation of a protein phosphatase cascade allows convergent dopamine and glutamate signals to activate ERK in the striatum. Proc Natl Acad Sci U S A. 2005 Jan 11; 102(2):491–6. [PubMed: 15608059]
35. Biever A, Puighermanal E, Nishi A, David A, Panciatici C, Longueville S, et al. PKA-dependent phosphorylation of ribosomal protein S6 does not correlate with translation efficiency in striatonigral and striatopallidal medium-sized spiny neurons. J Neurosci. 2015 Mar 11; 35(10): 4113–30. [PubMed: 25762659]
36. Krawczyk M, Georges F, Sharma R, Mason X, Berthet A, Bezard E, et al. Double-dissociation of the catecholaminergic modulation of synaptic transmission in the oval bed nucleus of the stria terminalis. J Neurophysiol. 2011 Jan; 105(1):145–53. [PubMed: 21047935]
37. Dufner A, Thomas G. Ribosomal S6 kinase signaling and the control of translation. Exp Cell Res. 1999 Nov 25; 253(1):100–9. [PubMed: 10579915]
38. Fadok JP, Darvas M, Dickerson TM, Palmiter RD. Long-term memory for pavlovian fear conditioning requires dopamine in the nucleus accumbens and basolateral amygdala. PLoS One. 2010; 5(9):e12751. [PubMed: 20856811]
39. Xu W, Sudhof TC. A neural circuit for memory specificity and generalization. Science. 2013 Mar 15; 339(6125):1290–5. [PubMed: 23493706]
40. Likhtik E, Stujenske JM, Topiwala MA, Harris AZ, Gordon JA. Prefrontal entrainment of amygdala activity signals safety in learned fear and innate anxiety. Nat Neurosci. 2014 Jan; 17(1): 106–13. [PubMed: 24241397]
41. Shaban H, Humeau Y, Herry C, Cassasus G, Shigemoto R, Ciocchi S, et al. Generalization of amygdala LTP and conditioned fear in the absence of presynaptic inhibition. Nat Neurosci. 2006 Aug; 9(8):1028–35. [PubMed: 16819521]
42. Li H, Penzo MA, Taniguchi H, Kopec CD, Huang ZJ, Li B. Experience-dependent modification of a central amygdala fear circuit. Nat Neurosci. 2013 Mar; 16(3):332–9. [PubMed: 23354330]

43. Wilensky AE, Schafe GE, Kristensen MP, LeDoux JE. Rethinking the fear circuit: the central nucleus of the amygdala is required for the acquisition, consolidation, and expression of Pavlovian fear conditioning. J Neurosci. 2006 Nov 29; 26(48):12387–96. [PubMed: 17135400]
44. LeDoux JE, Iwata J, Cicchetti P, Reis DJ. Different projections of the central amygdaloid nucleus mediate autonomic and behavioral correlates of conditioned fear. J Neurosci. 1988 Jul; 8(7):2517–29. [PubMed: 2854842]
45. Jennings JH, Sparta DR, Stamatakis AM, Ung RL, Pleil KE, Kash TL, et al. Distinct extended amygdala circuits for divergent motivational states. Nature. 2013 Apr 11; 496(7444):224–8. [PubMed: 23515155]
46. Kim SY, Adhikari A, Lee SY, Marshel JH, Kim CK, Mallory CS, et al. Diverging neural pathways assemble a behavioural state from separable features in anxiety. Nature. 2013 Apr 11; 496(7444): 219–23. [PubMed: 23515158]
47. Tye KM, Prakash R, Kim SY, Fenno LE, Grosenick L, Zarabi H, et al. Amygdala circuitry mediating reversible and bidirectional control of anxiety. Nature. 2011 Mar 17; 471(7338):358–62. [PubMed: 21389985]
48. Dong HW, Petrovich GD, Swanson LW. Topography of projections from amygdala to bed nuclei of the stria terminalis. Brain Res Brain Res Rev. 2001 Dec; 38(1–2):192–246. [PubMed: 11750933]
49. Dong HW, Petrovich GD, Watts AG, Swanson LW. Basic organization of projections from the oval and fusiform nuclei of the bed nuclei of the stria terminalis in adult rat brain. J Comp Neurol. 2001 Aug 6; 436(4):430–55. [PubMed: 11447588]
50. Nagy FZ, Pare D. Timing of impulses from the central amygdala and bed nucleus of the stria terminalis to the brain stem. J Neurophysiol. 2008 Dec; 100(6):3429–36. [PubMed: 18971295]
51. Haufler D, Pare D. High-frequency oscillations are prominent in the extended amygdala. J Neurophysiol. 2014 Jul 1; 112(1):110–9. [PubMed: 24717353]
52. Oh SW, Harris JA, Ng L, Winslow B, Cain N, Mihalas S, et al. A mesoscale connectome of the mouse brain. Nature. 2014 Apr 10; 508(7495):207–14. [PubMed: 24695228]
53. Bouthenet ML, Martres MP, Sales N, Schwartz JC. A detailed mapping of dopamine D-2 receptors in rat central nervous system by autoradiography with [125I]iodosulpride. Neuroscience. 1987 Jan; 20(1):117–55. [PubMed: 2882443]
54. Krawczyk M, Sharma R, Mason X, Debacker J, Jones AA, Dumont EC. A switch in the neuromodulatory effects of dopamine in the oval bed nucleus of the stria terminalis associated with cocaine self-administration in rats. J Neurosci. 2011 Jun 15; 31(24):8928–35. [PubMed: 21677176]
55. Naylor JC, Li Q, Kang-Park MH, Wilson WA, Kuhn C, Moore SD. Dopamine attenuates evoked inhibitory synaptic currents in central amygdala neurons. Eur J Neurosci. 2010 Dec; 32(11):1836–42. [PubMed: 20955472]
56. Penzo MA, Robert V, Tucciarone J, De Bundel D, Wang M, Van Aelst L, et al. The paraventricular thalamus controls a central amygdala fear circuit. Nature. 2015 Mar 26; 519(7544):455–9. [PubMed: 25600269]
57. Cai H, Haubensak W, Anthony TE, Anderson DJ. Central amygdala PKC-delta(+) neurons mediate the influence of multiple anorexigenic signals. Nat Neurosci. 2014 Sep; 17(9):1240–8. [PubMed: 25064852]
58. Botta P, Demmou L, Kasugai Y, Markovic M, Xu C, Fadok JP, et al. Regulating anxiety with extrasynaptic inhibition. Nat Neurosci. 2015 Oct; 18(10):1493–500. [PubMed: 26322928]
59. Mahler SV, Berridge KC. Which cue to “want?” Central amygdala opioid activation enhances and focuses incentive salience on a prepotent reward cue. J Neurosci. 2009 May 20; 29(20):6500–13. [PubMed: 19458221]
60. Blundell J, Kouser M, Powell CM. Systemic inhibition of mammalian target of rapamycin inhibits fear memory reconsolidation. Neurobiol Learn Mem. 2008 Jul; 90(1):28–35. [PubMed: 18316213]
61. Mac Callum PE, Hebert M, Adamec RE, Blundell J. Systemic inhibition of mtor kinase via rapamycin disrupts consolidation and reconsolidation of auditory fear memory. Neurobiol Learn Mem. 2014 Jul.112:176–85. [PubMed: 24012802]
62. Stoica L, Zhu PJ, Huang W, Zhou H, Kozma SC, Costa-Mattioli M. Selective pharmacogenetic inhibition of mammalian target of Rapamycin complex I (mTORC1) blocks long-term synaptic

plasticity and memory storage. Proc Natl Acad Sci U S A. 2011 Mar 1; 108(9):3791–6. [PubMed: 21307309]

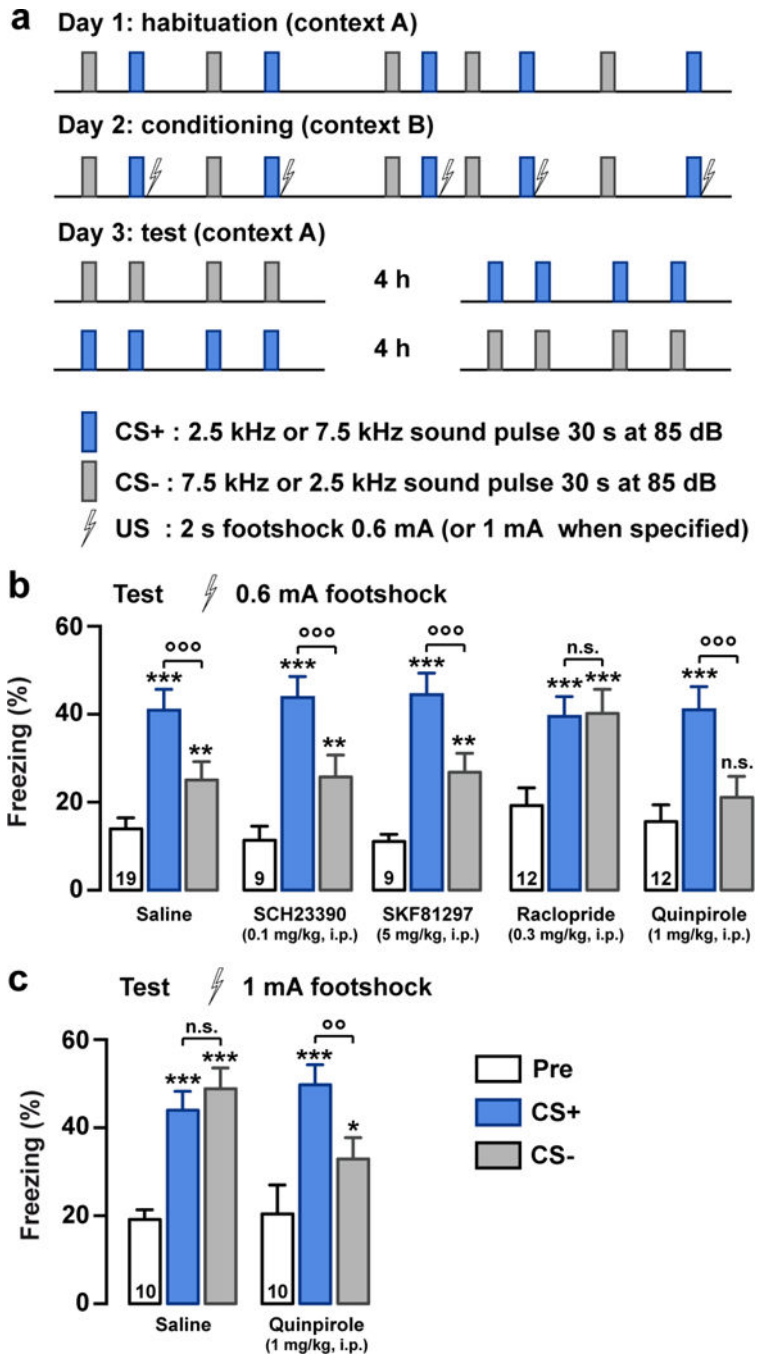

Figure 1. Bidirectional modulation of Pavlovian defensive reactions by dopamine D2R

(**a**) Protocol of discriminative auditory Pavlovian conditioning. (**b, c**) Freezing responses evoked by CS+ (blue bars) and CS− (grey bars) presentation in mice injected with saline, SCH29390 (0.1 mg/kg, i.p.), SKF81297 (5 mg/kg, i.p.), raclopride (0.3 mg/kg, i.p.) or quinpirole (1 mg/kg, i.p.) immediately after conditioning: pairings of sound cue with 0.6 mA (**b**) or 1 mA (**c**) foot shock. The average time spent freezing prior to presentation of the sounds during both test sessions (Pre, open bars) was used as a measure for contextual fear generalization. The number of animals in each condition is indicated in the bars. Values are

means + s.e.m. Statistical analysis, repeated measures ANOVA (values in Supplemental Table 1: 1b and 1c). Tukey's test, * $p < 0.05$, ** $p < 0.01$, *** $p < 0.001$ for comparison with Pre; °° $p < 0.01$, °°° $p < 0.001$ for comparison between CS+ and CS−.

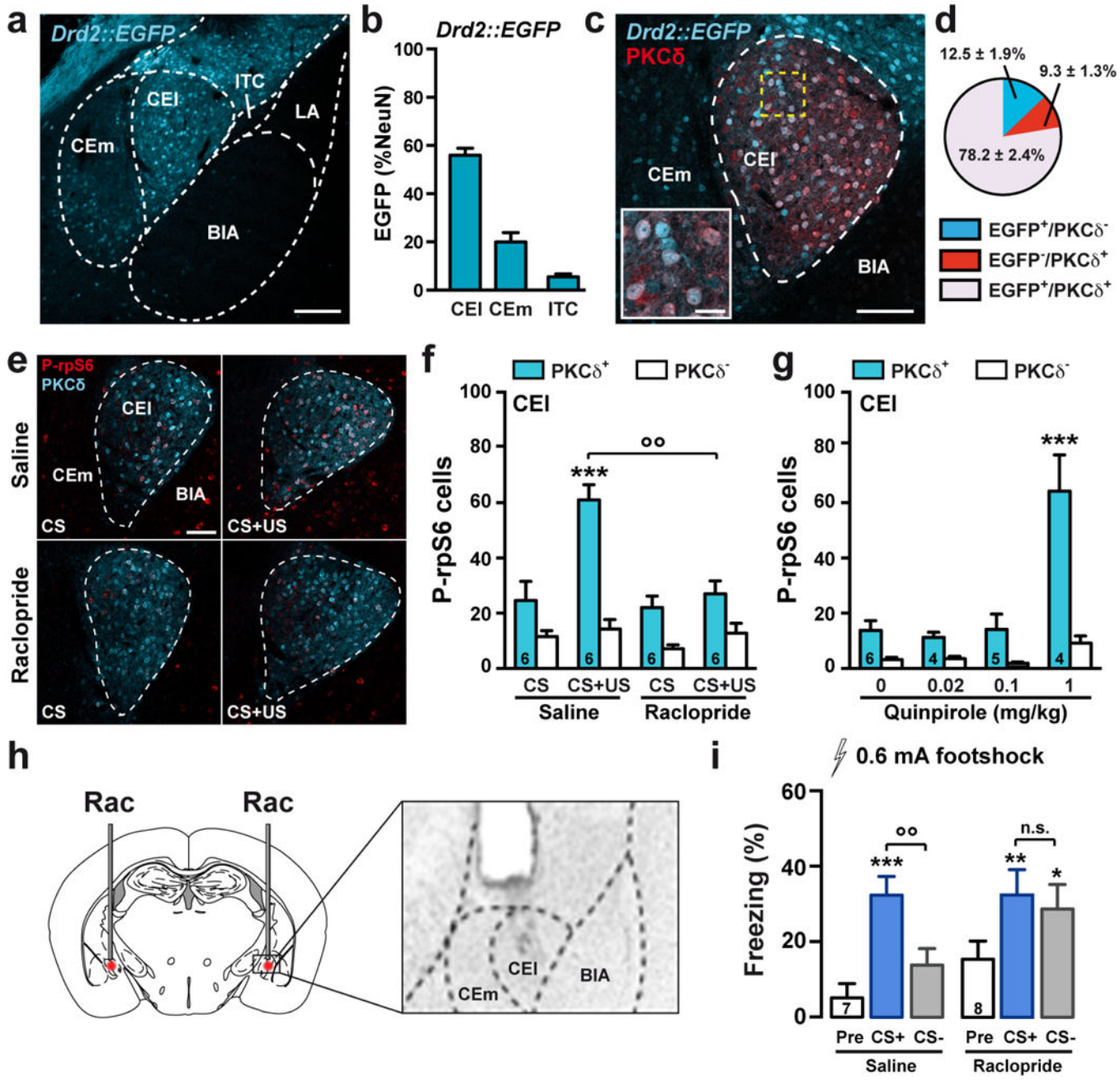

Figure 2. Blockade of D2R in the CEA induces generalized freezing responses

(**a**) Localization of D2R-expressing neurons in the CEA of *Drd2::EGFP* mice. Scale bar, 200 μm. (**b**) EGFP-positive neurons were quantified as a percent of NeuN-positive (not shown) cells 5 sections from 5 mice (**c**) Double immunostaining for EGFP (cyan) and PKCδ (red) in the CEl. Scale bar, 100 μm. Inset, high magnification of the area delineated by the yellow dashed line square. Scale bar, 25 μm. (**d**) Estimation of the proportion of D2R-containing neurons that express PKCδ in the CEl (1019 cells analyzed, n = 5 mice). (**e**) Immunofluorescence of P-rpS6 (red) and PKCδ (cyan) in the CEl 60 min after conditioning in mice injected with either saline or raclopride. Scale bar, 100 μm. (**f**) Number of P-rpS6-

positive cells in PKCδ$^+$ or PKCδ$^-$ neurons in the CEl of mice exposed to CS alone (white bars) or paired with US (cyan bars) and injected either with saline or raclopride. (**g**) Number of P-rpS6-immnopositive cells in PKCδ$^+$ or PKCδ$^-$ neurons in the CEl of mice receiving a single injection of quinpirole. (**h**) Schematic representation of the cannula placement for raclopride infusion into the CEA. (**i**) Freezing responses evoked by CS+ and CS− presentation in mice microinjected into the CEA with saline or raclopride immediately after conditioning: 5 pairings of sound cue with 0.6 mA foot shock. In (**f**), (**g**) and (**i**) the number of animals in each condition is indicated in the bars. Statistical analysis, two-way ANOVA or repeated measures ANOVA (values in Supplemental Table 1: 2f, 2g and 2i), Tukey's test in (**f**) *** $p < 0.001$ for comparison between CS and CS+US; °° $p < 0.01$, for comparison between saline and raclopride, in (**g**) *** $p < 0.001$ vs saline and in (**i**) * $p < 0.05$, ** $p < 0.01$, *** $p < 0.001$ for comparison with Pre; °° $p < 0.01$, for comparison between CS+ and CS−.

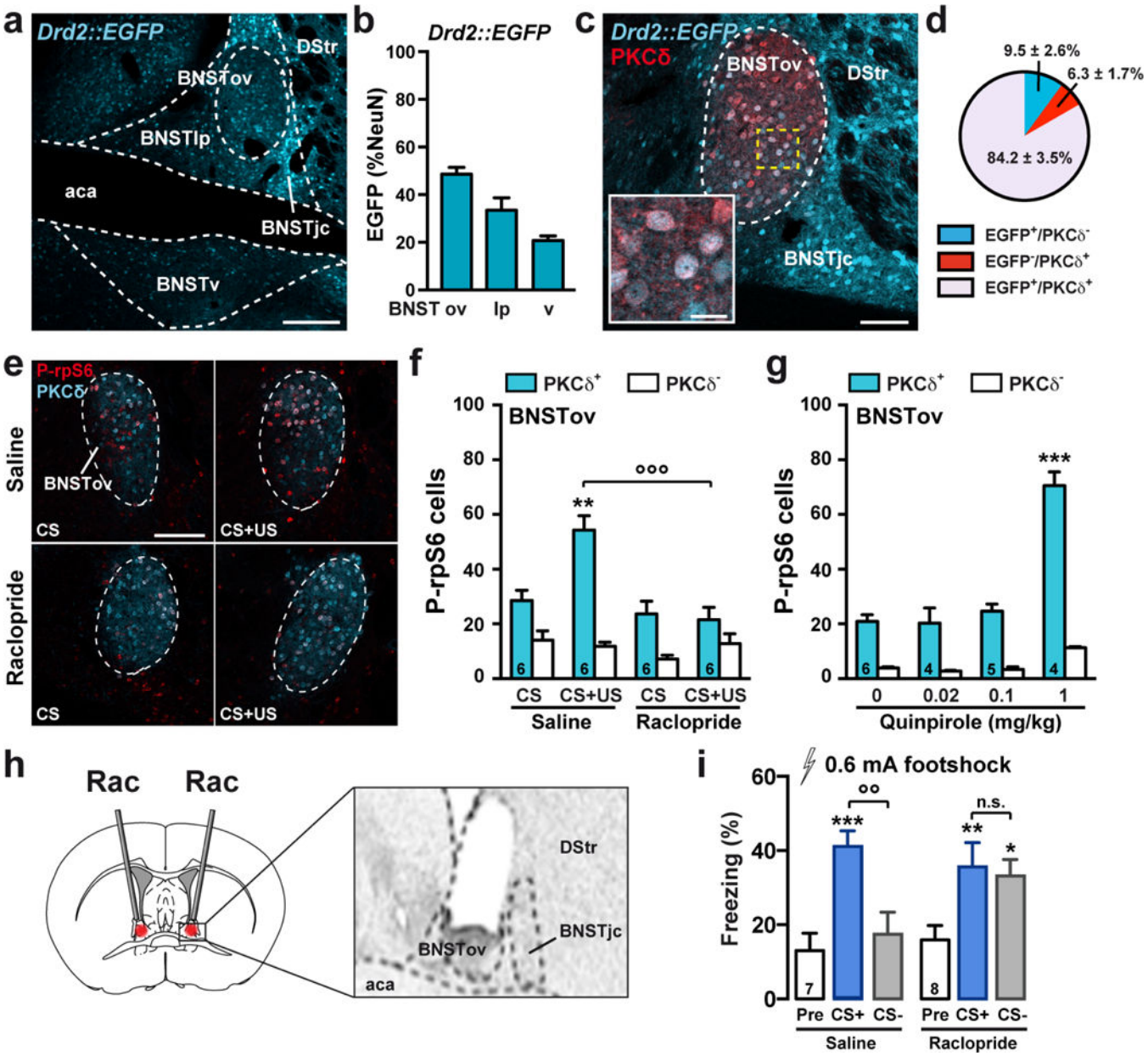

Figure 3. BNST D2R control fear generalization

(**a**) Localization of D2R-expressing neurons in the BNST of *Drd2::EGFP* mice. Scale bar, 200 μm. (**b**) EGFP-positive neurons were quantified as a percent of NeuN-positive (not shown) cells 5 sections from 5 mice. (**c**) Double immunostaining for EGFP (cyan) and PKCδ (red) in the BNSTov. Scale bar, 100 μm. Inset, high magnification of the area delineated by the yellow dashed line square. Scale bar, 20 μm. (**d**) Estimation of the proportion of D2R-containing neurons that express PKCδ in the BNSTov (*Drd2::EGFP*: 725 cells analyzed; n = 5 mice). (**e**) Immunofluorescence of P-rpS6 (red) and PKCδ (cyan) in the BNSTov 60 min after conditioning in mice injected with either saline or raclopride. Scale bar, 100 μm. (**f**) Number of P-rpS6-immunopositive cells in PKCδ^{+} or PKCδ^{-} neurons in the BNSTov of mice exposed to CS alone (white bars) or paired with US (cyan bars) and

injected either with saline or raclopride. (**g**) Number of P-rpS6-immunopositive cells in PKCδ^{+} or PKCδ^{-} neurons in the BNSTov of mice receiving a single injection of quinpirole. (**h**) Schematic representation of the cannula placement for raclopride infusion into the BNST. (**i**) Freezing responses evoked by CS+ and CS− presentation in mice microinjected with saline or raclopride immediately after conditioning: 5 pairings of sound cue with 0.6 mA footshock. In (**f**), (**g**) and (**i**) the number of animals in each condition is indicated in the bars. Statistical analysis, two-way ANOVA or repeated measures (values in Supplemental Table 1: 3f, 3g and 3i), Tukey's test in (**f**) ** $p < 0.01$ for comparison between CS and CS +US; ° $p < 0.05$, for comparison between saline and raclopride, in (**g**) *** $p < 0.001$ vs saline and in (**i**) * $p < 0.05$, ** $p < 0.01$, *** $p < 0.001$ for comparison with Pre; °° $p < 0.01$, for comparison between CS+ and CS−.

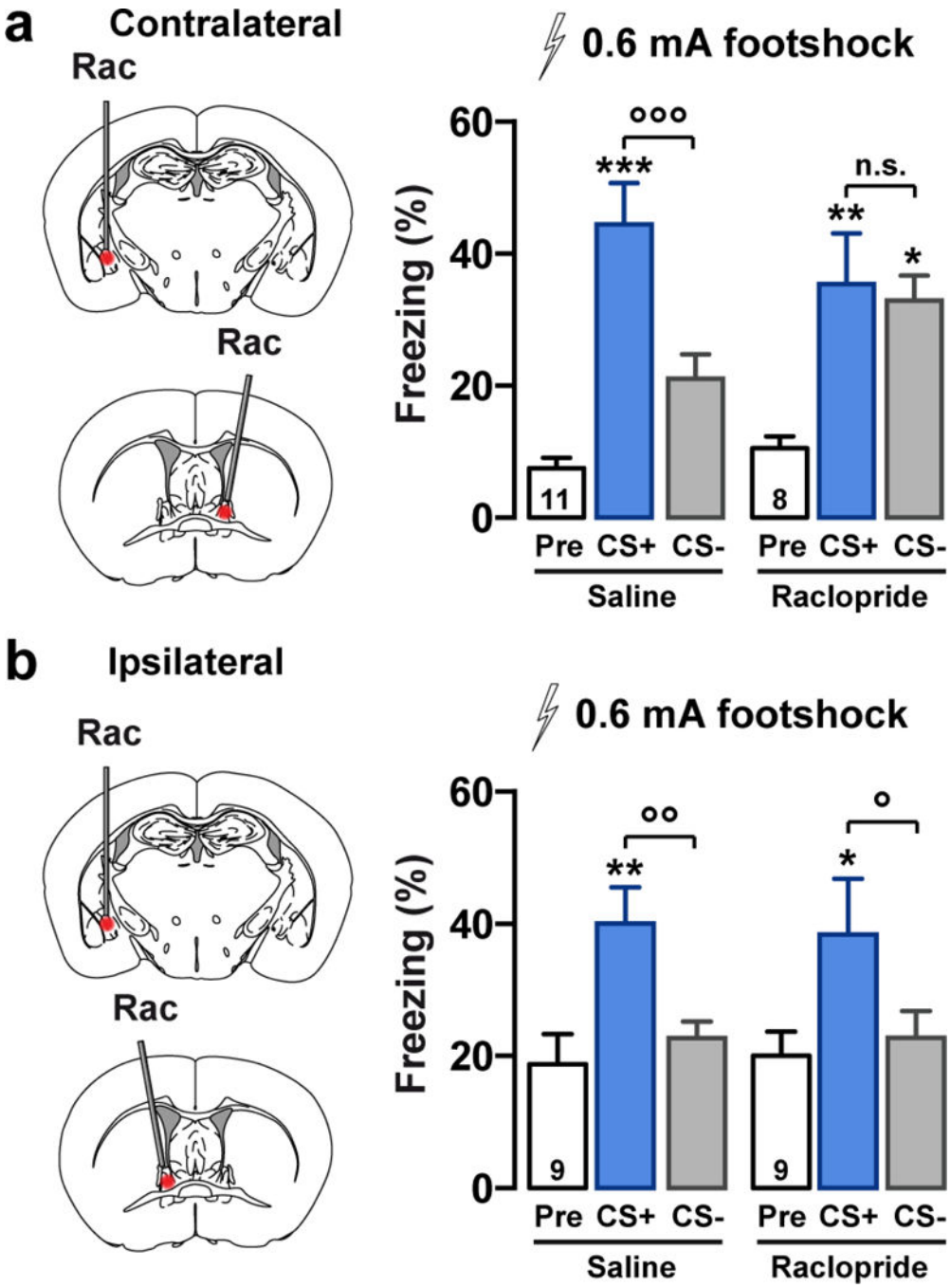

Figure 4. Concomitant D2R activation in the CEA and BNST prevents fear generalization

(**a**, **b**) Left panel, schematic diagram showing the location of raclopride infusion to block D2R into the CEA and BNST. (**a**) Right panel, contralateral raclopride infusions in the CEA and the BNST induce generalized freezing responses whereas ipsilateral infusions (**b**) do not (experiment replicated in three groups of animals). In (**a**) and (**b**) the number of animals in each condition is indicated in the bars and statistical analysis done with repeated measures (values in Supplemental Table1: 4a and 4b) and Tukey's test, * $p < 0.05$, ** $p < 0.01$, *** p

< 0.001 for comparison with Pre; ° $p < 0.05$, °° $p < 0.01$, °°° $p < 0.001$, for comparison between CS+ and CS−.

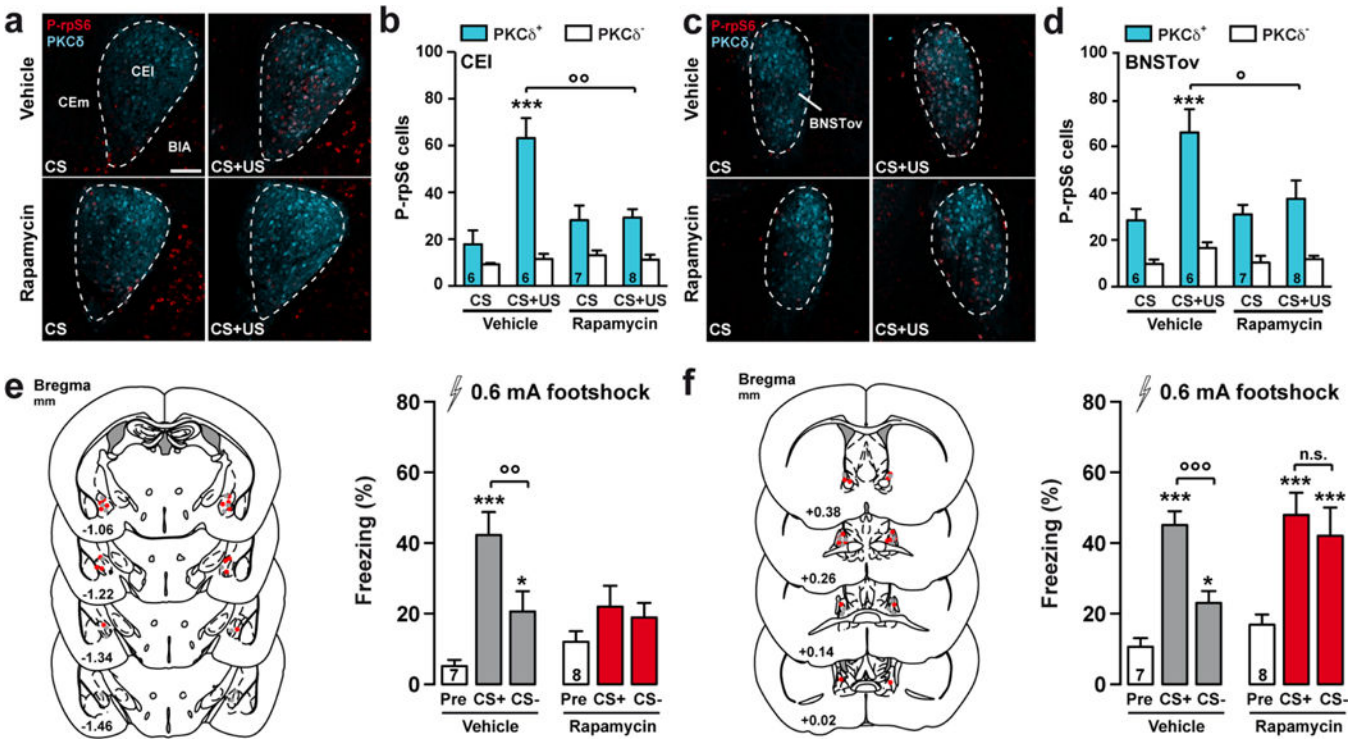

Figure 5. mTORC1 inhibition prevents rpS6 phosphorylation and induces generalization of defensive behavior

(**a**) Immunofluorescence of P-rpS6 (red) and PKCδ (cyan) in the CEl 60 min after conditioning in mice injected with either saline or rapamycin (5 mg/kg, i.p.). Scale bars, 100 μm. (**b**) Number of P-rpS6-positive cells in $PKC\delta^+$ or $PKC\delta^-$ neurons in the CEl of mice exposed to CS alone (white bars) or paired with US (cyan bars) and injected either with saline or rapamycin. *** $p < 0.001$ for comparison between CS and CS+US; ° $p < 0.05$, °° $p < 0.01$ for comparison between vehicle and rapamycin. (**c** and **d**) Same as in (**a** and **b**) for BNSTov. (**e**) Left panel, localization of cannula hits for bilateral infusion of rapamycin into the CEA. Right panel, freezing responses evoked by CS+ and CS−presentation in mice microinjected in the CEA with vehicle or rapamycin immediately after conditioning: 5 pairings of sound cue with 0.6 mA footshock. (**f**) same as in (**e**) for BNST. Mice microinjected with saline (grey dots) and rapamycin (red dots). * $p < 0.05$, *** $p < 0.001$ for comparison with Pre; °° $p < 0.01$, °°° $p < 0.001$, for comparison between CS+ and CS−. In (**b**), (**d**), (**e**) and (**f**), the number of animals in each condition is indicated in the bars and statistical analysis done by using two-way ANOVA or repeated measures (Values in Supplemental Table 1: 5b, 5d, 5e and 5f) followed by Tukey's test.